ADVANCES IN GEODESY AND GEOINFORMATION
(formerly GEODESY AND CARTOGRAPHY)
Vol. 72, no. 1, article no. e33, 2023

https://doi.org/10.24425/agg.2022.141919

Original paper

Monitoring of millimeter-scale deformations in Tallinn using repeated leveling and PS-InSAR analysis of Sentinel-1 data

Tõnis Oja*, Anti Gruno

Datel AS, Tallinn, Estonia
e-mail: tonis.oja@datel.ee; ORCID: http://orcid.org/0000-0001-9999-8525
e-mail: anti.gruno@value.space

*Corresponding author: Tõnis Oja, e-mail: tonis.oja@datel.ee

Received: 2022-08-17 / Accepted: 2022-10-14

Abstract: The aim of this study was to evaluate millimeter-scale deformations in Tallinn, the capital of Estonia, by using repeated leveling data and the synthetic aperture radar (SAR) images of Sentinel-1 satellite mission. The persistent scattered interferometric SAR (PS-InSAR) analysis of images from ascending and descending orbits from June 2016 to November 2021 resulted the line-of-sight (LOS) displacement velocities in the Tallinn city center. Velocity solutions were estimated for the full period of time, but also for shorter periods to monitor deformation changes in yearly basis. The gridded LOS velocity models were used for the decomposition of east-west and vertical velocities. Additionally, the uncertainty of 2D velocity solutions was estimated by following the propagation of uncertainty. The 3D velocity of permanent GNSS station "MUS2" in Tallinn was used to unify the reference of all PS-InSAR velocity solutions. The results of the latest leveling in Tallinn city center in 2007/2008 and 2019 showed rather small subsidence rates which were in agreement with InSAR long-term solution. However, the short-term InSAR velocity solutions revealed larger subsidence of city center with a rate about –10 mm/yr in 2016–2017, and the uplift around 5 mm/yr in 2018–2019 with relatively stable periods in 2017–2018 and 2019–2021. The inclusion of groundwater level observation data and the geological mapping information into the analysis revealed possible spatiotemporal correlation between the InSAR results and the groundwater level variations over the deep valleys buried under quaternary sediments.

Keywords: SAR interferometry, repeated leveling, vertical land movement, groundwater level change, geodetic network

1. Introduction

After the independence of Estonia in 1991, numerous construction works have been initiated in Tallinn, the capital of Estonia. The construction of new buildings has been most active in the city center. The construction activities need stable geodetic infrastruc-

ture (such as geodetic reference networks) for accurate land and construction surveying. The stability and accuracy of geodetic networks have to be monitored continuously by repeating high precision geodetic measurements on the network points. Such repeated terrestrial measurements are time and resource-consuming, especially when they are done over larger citywide or nationwide geodetic networks. Over the past few decades, space-borne multitemporal SAR interferometry (InSAR) has been developed as an alternative technique for the monitoring of land deformation (Crosetto et al., 2011) and thus also the stability of geodetic infrastructure. An important component of geodetic infrastructure is the physical height obtained from the geodetic leveling which is done relative to the reference surface such as a geoid/quasigeoid. In Estonia the nationwide height frame EH2000 (the national realization of the European Vertical Reference System) is based on a normal height concept (Estonian Ministry of Environment, 2017). The latest solution of the Tallinn height network followed the same concept and was connected to the EH2000 (Metricus, 2019).

The height benchmarks in Tallinn have been repeatedly measured during numerous leveling campaigns which were started more than 100 years ago (Kall and Torim, 2003). Several maps of vertical land movement (VLM) have been compiled on the basis of the results of repeated leveling (Zhelnin, 1958; Lutsar, 1965; Vallner and Lutsar, 1966; Kall and Torim, 2003). These VLM maps indicate the sinking of the Tallinn city center already in 1951. In 1960s, the highest subsidence rates up to 30 mm/yr were observed in Tallinn. From 1964 onwards, the sinking rate has been steadily decreasing (Lutsar, 1965). The data analysis by Kall and Torim (2003), based on the leveling done in 1986–2000, show that the sinking of the area that was being monitored, has stopped or reversed into rising. A correlation has been found between the leveling results, the geological structure and groundwater level changes (Vallner and Lutsar, 1966). Previous studies based on the historical repeated leveling performed in Tallinn, show largest VLM rates over the ancient valleys buried under quaternary sediments (Kall and Torim, 2003). In the Tallinn area several deep valley-like incisions with depths over 100 m exist, filled with glacial, glaciofluvial, glaciolacustrine deposits, and Holocene marine deposits (Vaher et al., 2010). According to the information obtained from the national geological base map, two buried valleys named as Lilleküla and Kadriorg exist in the analysis area of this study (Fig. 1).

The motivation of this study was to evaluate millimeter-scale deformations in the Tallinn city center with the help of the latest leveling and multitemporal InSAR analysis. In 2007–2008 and 2019 the height network in Tallinn was remeasured by using high precision leveling. The benchmarks common over these leveling campaigns are shown in Figure 1, and the measurements and results are introduced in Section 2. For InSAR analysis persistent scattered (PS-InSAR) technique and ESA Sentinel-1 satellite radar mission C-band images from ascending and descending orbits within 2016–2021 were used. Different orbits made possible to project the line-of-sight (LOS) measurements to vertical velocities, which were then used to monitor the benchmark stability of the city's height network. Moreover, the geological information about buried valleys and the water level measurements from groundwater wells in the Tallinn area (see Fig. 1) were included into the current analysis to investigate the connection between the VLM, geology and groundwater level.

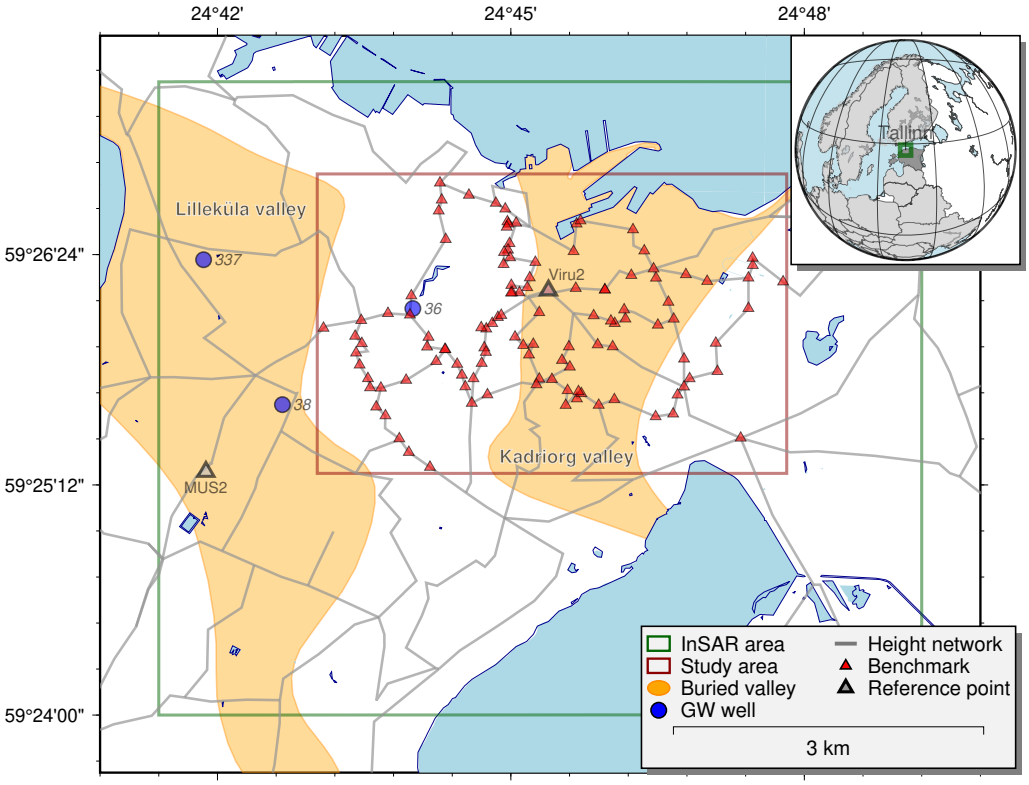

Fig. 1. A larger computation area was selected for InSAR analysis which contains a smaller study area with the benchmarks and leveling lines of Tallinn height network leveled in 2007–2019. The analysis area in Estonia (with darker gray) as a part of the European Union (with lighter gray) is shown on the upper right corner. The geodetic reference points used in the analysis of this study are shown as well. The spatial data about buried valleys and groundwater wells were requested respectively from the public databases (KESE, 2022; XGIS, 2022)

2. Leveling data

Two precise leveling campaigns of the Tallinn height network undertaken in 2007/2008 and 2019 were used in the current analysis (Fig. 2). Trimble DiNi 12 digital levels and the calibrated invar leveling staffs with temperature sensors were used during the campaigns. The field data were later corrected for the temperature and scale change of staffs, gravity field variations and the land uplift (Gruno, 2020). The network adjustment solutions of first and second leveling resulted the height values for 116 common benchmarks with mean uncertainty of ±0.23 mm and ±0.31 mm (1-sigma), respectively. The majority of the leveled points were the wall benchmarks (95), mounted in a building's foundation. The other leveled points were ground benchmarks (10), geodetic points (9) and deep seated, so-called fundamental benchmarks (2). A fundamental benchmark "Viru2" with ID number 63-843-99004 (GPA, 2022) was used to fix the network adjustment. From

the height differences between two adjusted network solutions over the time period of 12 years the velocity values of the benchmarks with mean uncertainty of ±0.03 mm/yr were estimated.

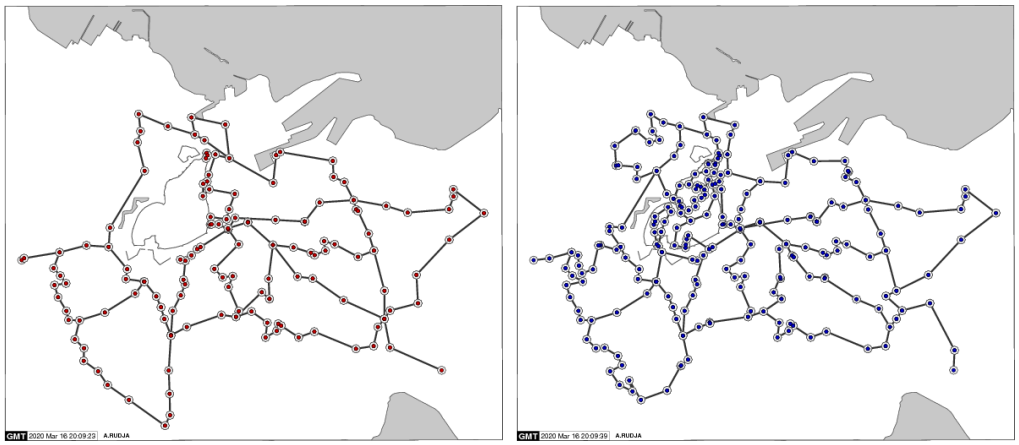

Fig. 2. Precise leveling campaigns of the Tallinn height network undertaken in 2007/2008 and 2019. The networks were adjusted separately to obtain height values at leveled benchmarks. Height differences and velocities were then calculated for the 116 common benchmarks

3. InSAR analysis

After the selection of analysis area in Tallinn and Sentinel-1 orbits, the satellite-based monitoring service SILLE (www.sille.space) automatically downloaded all Sentinel-1A/B IW SLC images from the public servers. For the multitemporal InSAR analysis the method based on the persistent scatterers (PS) by Ferretti et al. (2001) was applied to analyze SAR images. The software SARPROZ was used to compute the time series of LOS displacements and to estimate velocities at the PS points (Perissin et al., 2011). The software automatically downloaded precise orbits for each image. The DTM with 10 m × 10 m resolution was applied for the removal of topographic phase components which is the product of precise airborne LIDAR measurements done by the Estonian Land Board and was downloaded from geoportaal.maaamet.ee. The baseline configuration relative to the single-master image was formed, with interferometric pairs between the master and slave images. The selection of PS points (pixels) to filter high quality results was based on the value of amplitude stability index (*ASI*), spatial and temporal coherences (*sCoh*, *tCoh*) estimated for every processed pixel. The atmospheric phase screen (APS) was estimated by setting a linear velocity model at selected PS where a threshold value of the combined $ASI + sCoh$ of 1.6 was used. After the removal of the APS part the velocity of PS points and its uncertainty were estimated by applying a linear deformation model. Only pixels with $ASI + sCoh > 1.4$ was used as input of InSAR analysis. For the output only pixels with *tCoh* over 0.7 were selected.

In total, 237 images from the descending orbit (DESC with relative number #80, incidence and azimuth angles 43.52° and 189.4°, respectively) and 250 images from ascending orbit (ASC #160 with 33.54° and 348.0°) from June 2016 to November 2021 were used in the PS-InSAR analysis (Table 1). The displacement velocities of PS targets along the line-of-sight (LOS) from the stacks of 45–60 images were also estimated for shorter periods to monitor deformation changes on a yearly basis. Although the time series of Sentinel-1 images started already from 2014, there is a significant data gap from late October 2015 to early June 2016. To avoid the loss of temporal coherence between the SAR images due to the gap, no images before June 2016 were used in the following analysis.

Table 1. The parameters of different Sentinel-1 orbits for the long period of time (2016–2021) and the short, mostly yearly periods

Rel. orbit no.	Pass	Time period	No. of images	Orbital parameters	
				Incidence (°)	Azimuth (°)
80	DESC	08.07.2016–09.11.2021	237	43.4441	189.3921
		14.06.2016–06.11.2017	58	43.5179	189.3537
		06.11.2017–01.11.2018	46	–	–
		01.11.2018–02.11.2019	45	–	–
		02.11.2019–08.11.2020	47	–	–
		08.11.2020–09.11.2021	46	43.5046	189.3587
160	ASC	01.07.2016–08.11.2021	250	33.5513	348.1109
		07.06.2016–05.11.2017	60	33.5389	347.9874
		05.11.2017–06.11.2018	50	–	–
		06.11.2018–01.11.2019	48	–	–
		01.11.2019–07.11.2020	48	–	–
		07.11.2020–08.11.2021	49	33.5513	348.1109

As a result, about 32000 data points with LOS velocities and their uncertainties were determined in the PS-InSAR analysis of ASC, DESC radar images for the time period from June 2016 to November 2021. The mean velocity was close to zero with minimum –13 mm/yr and maximum +4 mm/yr. The mean uncertainty of LOS velocities was ±0.46 mm/yr (minimum equal to ±0.42 mm/yr, maximum equal to ±0.87 mm/yr). The analysis of shorter time periods resulted in a much higher LOS velocity range from –25 to 10 mm/yr. However, also the noise level increased as the mean uncertainty of the short-term velocity solutions was about 2 mm/yr. The LOS displacements, velocities and pointwise time-series were also presented through the map interface of SILLE (Fig. 3 and Fig. 4).

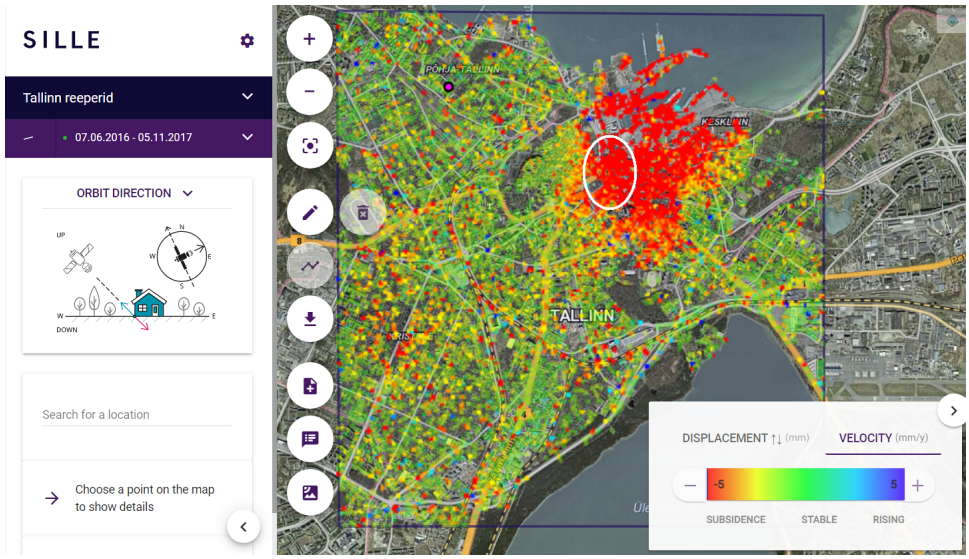

Fig. 3. LOS velocities of PS points in Tallinn presented through SILLE web service as a result of PS-InSAR analysis of SAR images from ASC orbit (#160), collected between June 2016 and November 2017

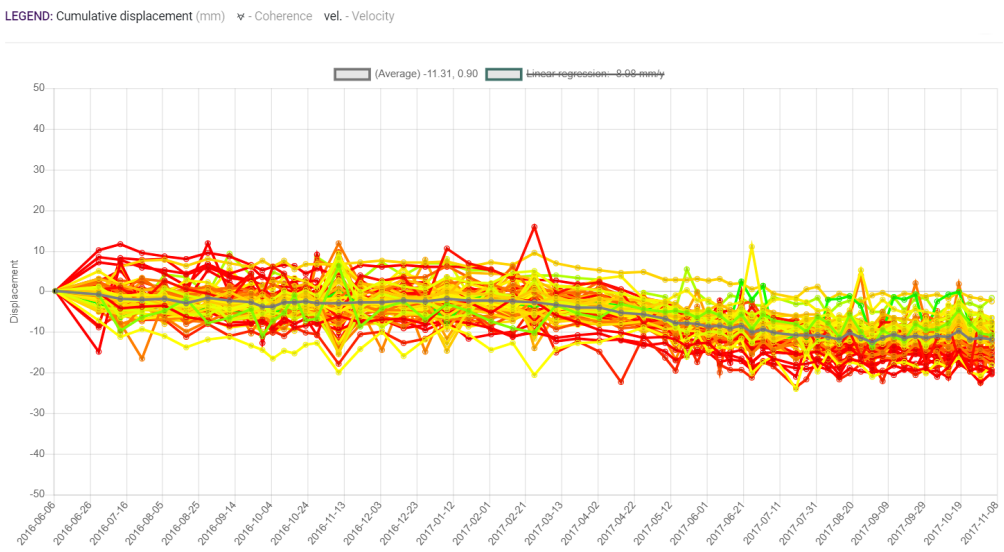

Fig. 4. LOS displacement time series of selected PS points (marked by white ellipse in Fig. 3) as a result of PS-InSAR analysis of SAR images from ASC orbit (#160) between June 2016 and November 2017

4. Decomposition of LOS velocities

The LOS velocities derived from the ASC and DESC nearly polar orbits provided sufficient information to calculate the horizontal (east-west) component as well as vertical component of the displacement velocity vector. The gridding of point velocities (by using

2D splines) resulted LOS velocity models which then were used to estimate the horizontal and vertical velocity models. Due to the different reference points of LOS velocities (from ASC, DESC orbits) used in PS-InSAR analysis, the unification to a common reference velocity was needed. The 3D velocity of permanent GNSS station "MUS2" in Tallinn was applied to unify reference of all LOS velocity solutions.

For the evaluation of benchmark stability and further comparison of vertical velocities, the LOS velocity is decomposed into the horizontal and vertical velocity components. The trigonometric relation between one dimensional (1D) LOS velocity vector (denoted as v_L) and the north-south, east-west and vertical components (denoted as v_N, v_E, v_H, respectively) of 3D velocity vector on the Earth's surface is following:

$$v_L = v_N \cdot \sin\alpha \cdot \sin\theta - v_E \cdot \cos\alpha \cdot \sin\theta + v_H \cdot \cos\theta, \tag{1}$$

where θ is the incidence angle (the angle between the local zenith and the looking vector of the satellite) and α is the azimuth angle measured clockwise relative to the north (see e.g. Fuhrmann and Garthwaite, 2019). These angles were given as orbital parameters in Table 1. The decomposition of 1D LOS velocity into the 3D velocity components by Eq. (1) can be done by solving the linear system, in which at least three LOS velocity solutions from different orbits are needed. However, the v_L values from two different opposite ASC, DESC orbits (marked as v_{L1}, v_{L2}) allows to estimate only two components of 3D vector. Due to the near polar orbit of Sentinel-1 the sensitivity for the detection of movements along north-south direction is limited (Fuhrmann and Garthwaite, 2019). Thus the v_N component is excluded from the decomposition given by Eq. (1). The decomposition from LOS to 2D velocity is done by solving the linear system:

$$\begin{bmatrix} v_E \\ v_H \end{bmatrix} = \begin{bmatrix} -\cos\alpha_1 \cdot \sin\theta_1 & \cos\theta_1 \\ -\cos\alpha_2 \cdot \sin\theta_2 & \cos\theta_2 \end{bmatrix}^{-1} \begin{bmatrix} v_{L1} \\ v_{L2} \end{bmatrix} = M^{-1} \begin{bmatrix} v_{L1} \\ v_{L2} \end{bmatrix}, \tag{2}$$

where the M^{-1} is the inverse of transformation matrix M.

Another issue with LOS decomposition is the different locations of PS points from different orbits, i.e. PS points from ASC orbit ($L1$) do not overlap spatially with PS points from DESC orbit ($L2$). Our solution to overcome that issue was the gridding of irregularly spaced LOS point to the gridded velocity models.

The Generic Mapping Tools (GMT) software was used for the gridding process (Wessel et al., 2019). Firstly, a mean value for every non-empty block in a grid region was computed by using GMT *blockmean*. The suitable block size with dimensions dLon/dLat = $1.44''/0.72'' = 0.0004°/0.0002°$ (about 23/22 m on a plane) was determined from the analysis of spatial data density. Weighted mean values for each block were computed by using the velocity uncertainties (v) to construct the weight = $1/u(v)$. Such an averaging before the grid modeling is recommended to avoid spatial aliasing due to the short wavelength information in data (GMT, 2021). Secondly, GMT *surface* was used to convert irregular, randomly spaced input data to a regular binary grid by using continuous curvature 2D splines with adjustable tension (Smith and Wessel, 1990). The latter was adjusted by changing the tension factor T value between 0 and 1. For the current

analysis $T = 0.3$ was selected. For the grid nodes with a distance more than 300 m from the nearest PS points, a value was set to NaN (Not-a-Number) to avoid the propagation of interpolation errors in these nodes (Fig. 5). After gridding step, the gridded LOS velocities were converted to E, H grids by using the relation Eq. (2). Additionally, the variance grids of E, H components were estimated by gridding the variance of LOS velocities $\mathrm{Var}(v_L)$ with the method described above, and by following the propagation of uncertainty (JCGM, 2011):

$$\begin{bmatrix} \mathrm{Var}(v_E) \\ \mathrm{Var}(v_H) \end{bmatrix} = M^{-1} \begin{bmatrix} \mathrm{Var}(v_{L1}) \\ \mathrm{Var}(v_{L2}) \end{bmatrix} \left(M^{-1}\right)^T, \tag{3}$$

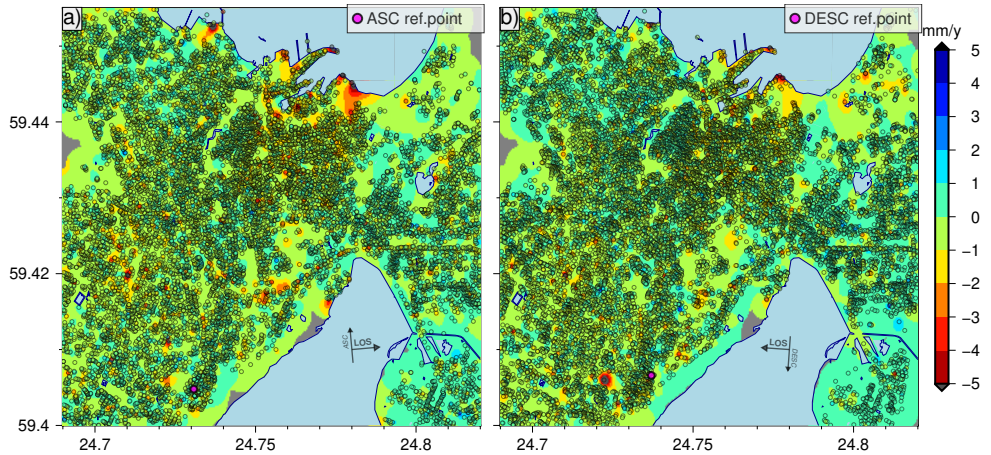

Fig. 5. Gridded LOS velocity solutions (2016–2021) with PS points from the ascending (left) and descending (right) orbits. For the grid nodes with a distance more than 300 m from the nearest PS points, no values were computed (marked as gray area)

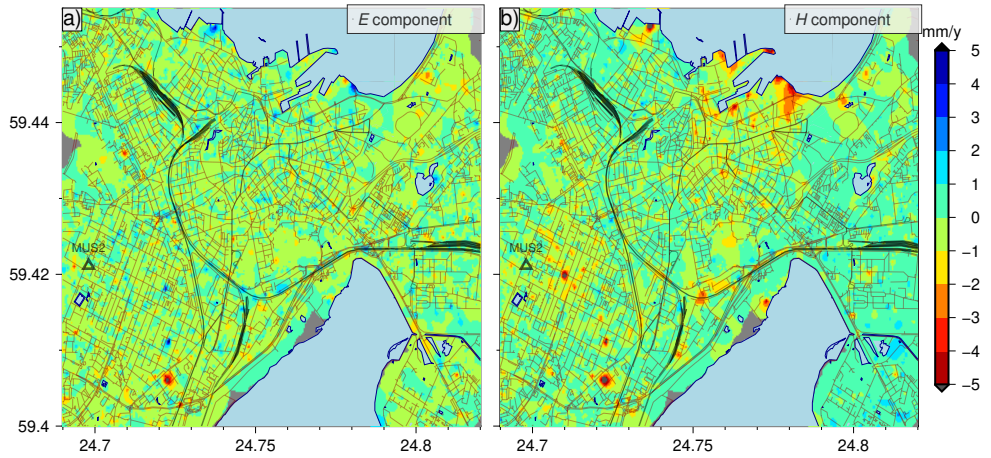

Fig. 6. Velocity solutions for east-west (E) and vertical (H) components (2016–2021) decomposed from the LOS velocities. The solutions have been fixed at the location of permanent GNSS stations "MUS2" (for more information see text)

where the uncertainty of velocity $u(v)$ is found from the variance $u(v) = \sqrt{\mathrm{Var}(v)}$ (Fig. 7). The uncertainties of vertical velocities turn out to be useful component in the data analysis below.

According to the purpose of the paper only the vertical velocity solutions over shorter, yearly time periods are shown in Figure 8. The results revealed strong subsidence signal

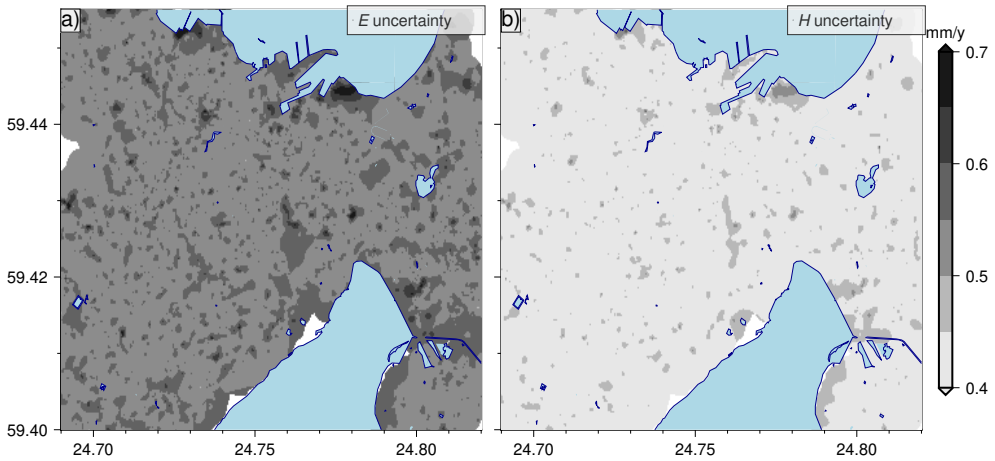

Fig. 7. Uncertainty grids of E, Hvelocity solutions (2016–2021) derived from the standard deviations of LOS velocities by using Eq. (3)

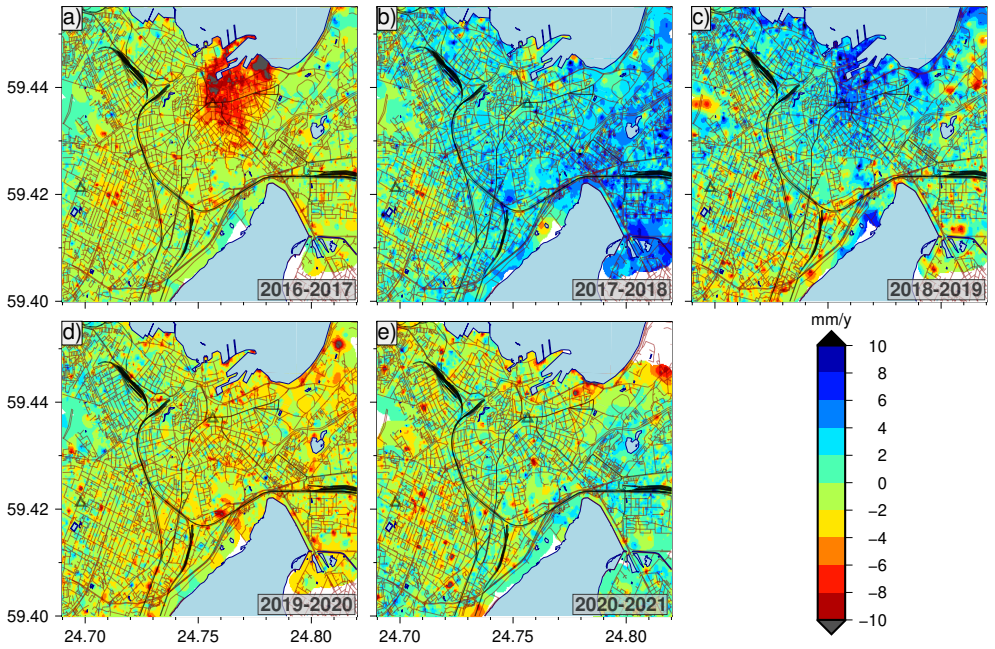

Fig. 8. A series of vertical velocity models from yearly InSAR analyses to monitor short-term deformation changes in Tallinn city center

in 2016–2017 and uplift in 2018–2019. The velocity range of short-term solutions is 2–3 times higher (about –25 to 11 mm/yr) than the velocities over longer time period (from –13 to 3 mm/yr, see Fig. 6b). However, also the noise level of yearly velocity solutions increases considerably. The mean uncertainty of vertical velocity models for short and long time periods are ±2.10 mm/yr and ±0.43 mm/yr, respectively.

5. Selection of reference point

In general, the location of a reference point (RP) is different across different InSAR analyses. It is due to the selection algorithm used to find suitable RP in InSAR analysis which is based on the statistics of PS points. By choosing different RP location the reference velocity of PS-InSAR solutions changes, and thus, the velocity solutions with different RP are not comparable. The same conclusion is valid also for the E, H velocity solutions, see Eq. (2). To make velocities comparable, we chose a common RP for all solutions. Velocity models were then shifted by a constant value so that the velocity became zero ($v_{2D} = 0.0$ mm/yr) at the location of common RP. It is noted that for the estimation of velocity value from a grid to a specific location (e.g. to RP) here and in the following analysis, a bicubic interpolation method with antialiasing has been applied by using GMT *grdtrack* (GMT, 2021).

Several criteria can be followed by selecting suitable RP. In current case the position of permanent GNSS station (pGNSS) "MUS2" in Tallinn with ID number 63-834-5468 and coordinates of Lat = 59.42115°, Long = 24.69803° was chosen for RP (GPA, 2022). The pGNSS station "MUS2" operated by the Estonian Land Board since 2008 has long measurement history and also good stability of the site has been found from the time series analysis. For instance, from the data processing of "MUS2" coordinates in 2012–2021 the velocities $v_E = -0.17 \pm 0.19$ mm/yr and $v_H = 3.14 \pm 0.79$ mm/yr in the global reference frame IGS14 have been estimated by the Nevada Geodetic Laboratory (NGL, 2021). The vertical component clearly shows the effect of postglacial rebound, a known secular signal in Northern Europe. This regional signal can be accurately predicted by the contemporary uplift model NKG2016LU_ABS (Vestøl et al., 2019). According to the NKG2016LU_ABS the vertical velocity (in the global reference frame ITRF2008) at the location of "MUS2" is $v_H = 3.19 \pm 0.16$ mm/yr. Although the comparison of velocities in different reference frames might introduce a small systematic bias, such a good agreement between the modeled and measured velocities indicated that no significant local signal disturbs the motion of "MUS2". In other words, the selected RP position is locally stable. Additionally, the selection of one or several pGNSS as a reference makes it possible to convert InSAR velocities to the global reference frame (such as ITRF2008 or IGS14 mentioned above, or the latest ITRF2020) which could be useful for nationwide or international researches and applications. Of course, the assumption about the scale and the orientation of InSAR velocity vectors aligned with global reference frame has to be made as well.

However, for the comparison at the height network it is also important to consider the InSAR derived vertical velocities at the location of reference benchmark (rBM) of the

repeated leveling in Tallinn. The interpolation revealed that the vertical velocity value from the solution of 2016–2021 is −0.4 mm/yr at the rBM "Viru2". This bias in the reference velocity value is slightly less than the mean uncertainty of vertical velocities derived from InSAR data, and thus, it can be regarded as statistically non-significant in the following comparisons. For short-term InSAR velocity solutions the bias at the rBM is higher and varies from −4.3 mm/yr to 4.7 mm/yr. The reason of such a variation is seen in Figure 7, whereas at the location of rBM in Tallinn city center the strong subsidence signal appeared in 2016–2017 followed by the uplift event in 2018–2019. In summary, the reference velocity of rBM is strongly influenced by local annual movements and the location of pGNSS "MUS2" over rBM was preferred as a stable RP to fix InSAR velocity solutions.

6. Comparison at the benchmarks

For the evaluation of height network stability in Tallinn the velocities at the location of benchmarks were interpolated from all InSAR vertical velocity solutions (Fig. 9 and Fig. 10). The InSAR velocities from long-term solution were compared with the leveled velocities at the benchmarks to determine statistically significant differences. Broadly, the leveling and InSAR velocities are mostly below 2 mm/yr and match well (Fig. 10).

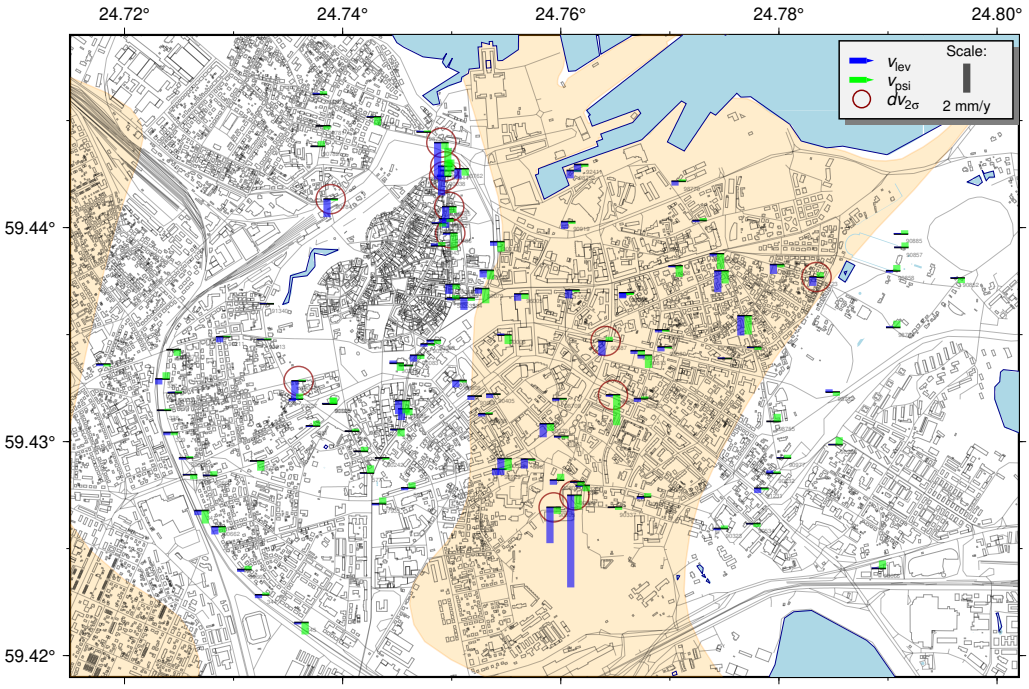

Fig. 9. The comparison of the leveled (2007–2019) and InSAR velocities (2016–2021) at the benchmarks of Tallinn height network. The benchmarks with significant differences ($dv_{2\sigma}$) between leveled and InSAR results by following the 2σ rule are circled

At the benchmarks where leveled or InSAR velocities are higher than 2 mm/yr, also larger differences between velocity solutions are visible. To test the statistical significance of velocity difference:

$$dv = v_{sar} - v_{lev}, \tag{4}$$

the standard uncertainty estimates given above (see Sections 2 and 4) were used to estimate the standard uncertainty of difference $u(dv)$. As $u(v_{\mathrm{sar}})$ is order of magnitude higher than $u(v_{\mathrm{lev}})$, the former dominates in $u(dv)$ value. Accordingly, for 2016–2021 $u(dv) = \pm 0.43$ mm/yr and for annual periods the corresponding value is about ± 2.10 mm/yr.

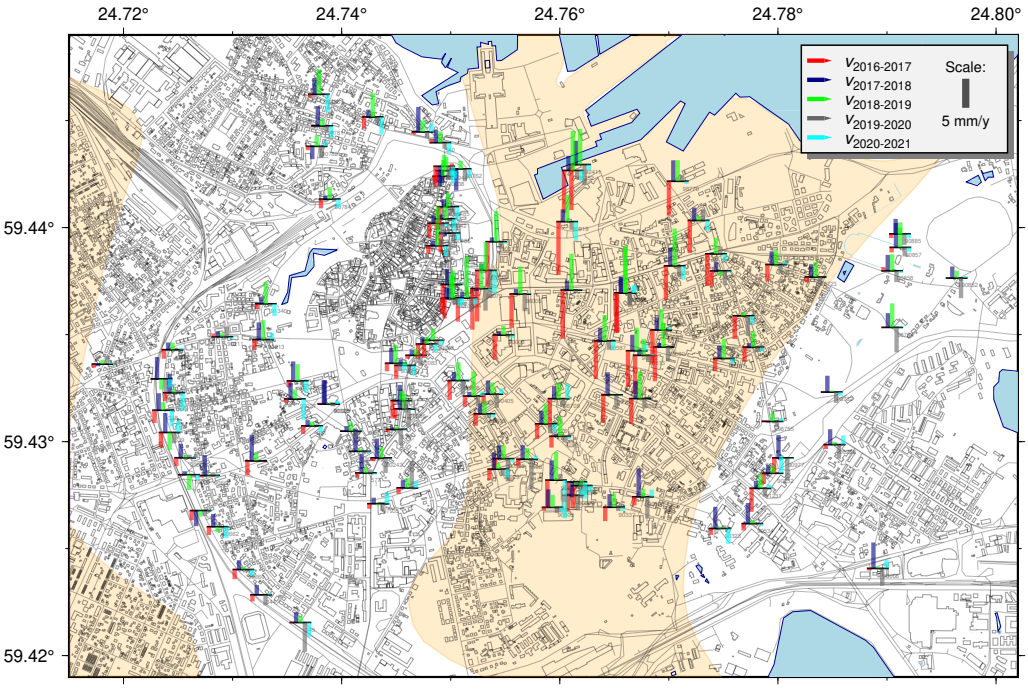

Fig. 10. Velocities from yearly InSAR solutions at the benchmarks of Tallinn height network

By assuming the normal distribution of leveling and InSAR observations, the statistical significance of the differences between the leveled and InSAR derived vertical velocities were tested within 1σ, 2σ and 3σ confidence intervals (with confidence level 68.3%, 95.5% and 99.7%, respectively). We found that within 1σ, 2σ and 3σ intervals the differences are not statistically significant at 70 benchmarks (60% of all benchmarks), 104 benchmarks (90%) and 108 benchmarks (93%), respectively. Correspondingly, the differences were found to be statistically significant for 46 benchmarks (40%), 12 benchmarks (10%) and 8 benchmarks (7%). The benchmarks with significant differences within 2σ confidence interval are marked by circle in Figure 9.

The yearly InSAR solutions confirm the findings of Figure 8, by revealing strong subsidence in 2016–2017 (marked by red bars in Figure 10) and the following uplift at the benchmarks in the city center (blue, green bars). Furthermore, the results suggest

that subsidence process in the city center is not fully recovered by the uplift, since the negative velocity values in 2016–2017 numerically exceed the positive values measured after 2017. Different movement patterns and also much smaller velocities of benchmarks can be seen outside the city center.

7. Discussion

The long and short-term vertical velocity solutions from InSAR analyses have been unified by using the same RP (pGNSS "MUS2") which makes these results comparable. Different RP has been used for the leveled vertical velocities (see Section 2), and thus one may argue about the comparability of leveled and InSAR velocity solutions (Fig. 9). However, we should keep in mind that both the leveling and InSAR are relative measurement methods, and therefore the selection of RP is quite arbitrary. For instance, in Figure 8 it is possible to find a benchmark where velocities from different solutions are equally close to zero. Now we can temporary select this benchmark as a new RP which makes solutions still comparable relative to this temporarily selected benchmark.

Another issue with the comparison of leveled and InSAR movements arose when different spatial and temporal domain and resolution of measured data were considered. Understandably, two leveling campaigns separated by 12 years could be only used to monitor long-term, decadal trend. At the same time, the impact of upward-downward movements detected by the InSAR analysis (see Fig. 8 and Fig. 10) is anticipated on leveled results. For example, the uplift of city center, and thus also rBM, up to 5–6 mm/yr during the leveling campaign in 2019 should result negative leveled velocities with same magnitude around the city center due to rising reference. Although negative leveled velocities prevail (Fig. 9), no clear subsidence pattern of benchmarks around the city center was detected. It could be that the second leveling took place after the uplift event in 2018–2019 and thus no considerable influence on leveled results was found. It is also noted here that the foundation of rBM is at the depth of 46.44 m from the ground (GPA, 2022) and is insulated from the upper geological layers, therefore it might be less influenced by the VLM linked with hydrogeological process discussed further.

The historical studies based on the repeated leveling (see Section 1) have shown that the local vertical movements in Tallinn were linked with the deep buried valleys filled with Quaternary sediments.

Furthermore, a correlation between the leveled subsidence rates and the groundwater level depletion was noticed over these buried valleys, due to the compaction of sediment layers. Supposedly, a similar correlation is expected with vertical velocities obtained from InSAR analysis. The polygons of two buried valleys (Lilleküla, Kadriorg) and the groundwater level data of three wells (with ID numbers 36, 38, 337) in Tallinn area were retrieved from the national geological base map (XGIS, 2022) and the environmental monitoring information system (KESE, 2022), respectively (see also Fig. 1). The groundwater level of the Cambrian-Vendian aquifer system was monthly measured in the wells 36 (the aquifer system is denoted as Cm-V) and 38 (denoted as V2gd). The groundwater level of the Quaternary aquifer (denoted as fQIII) was observed in the well

337. Two wells (38, 337) are positioned in the area over the Lilleküla buried valley, and well 36 is located on the slope of Toompea bedrock hill near the city center, between the Lilleküla and Kadriorg buried valleys. Unfortunately, no groundwater level monitoring wells were found in the city center and over the Kadriorg buried valley, where the largest displacements were detected.

The groundwater level variations observed in the wells from 2015 to 2022 indicated a clear temporal coherence with vertical movements in the Tallinn city center. The drop about 2–2.5 m of groundwater level in 2016 occurred at the same time with the subsidence of the city center with the rate 10 mm/yr or even more. After the lowest values two years later the water level started to increase around 1 m and was stabilized in 2020–2022 (Fig. 11). The short-term InSAR velocity solutions showed quite a stable period in 2017–2018, followed by the land uplift of 5–10 mm/yr in 2018–2019 and another stability period later on (Fig. 8 and Fig. 10). It can also be seen that the groundwater level has not fully recovered to the initial level, and same is true for the vertical displacements – the magnitude of the subsidence rates are mostly greater than the following uplift rates. As a conclusion, the recovery of groundwater level and also the uplift to the initial position might not yet be completed in Tallinn city center. It is a challenging question for the future, is the recovery process continuing (to the initial position) or is it actually completed (to the new stability position). New InSAR data complemented with terrestrial

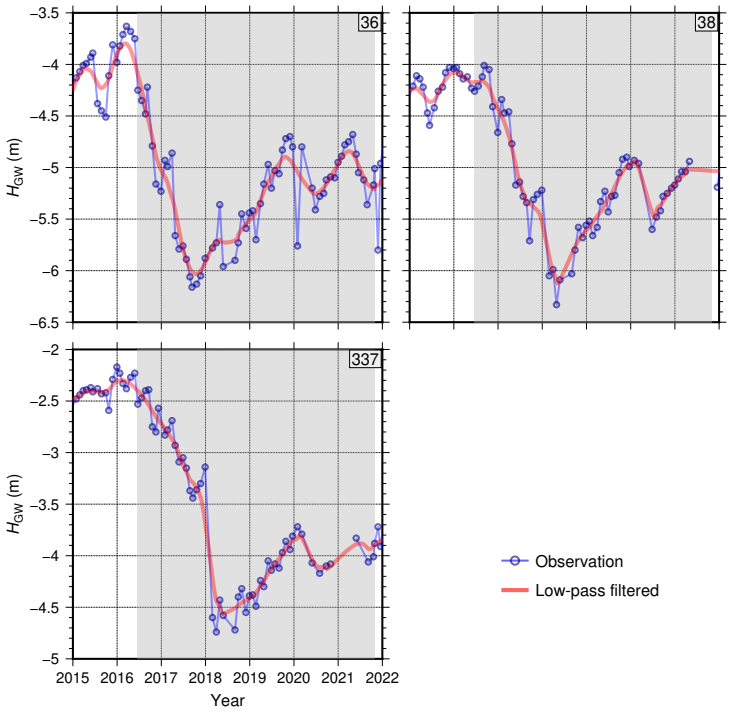

Fig. 11. Groundwater level variations of wells with ID numbers 36, 38 and 337 in Tallinn within 2015–2022 (KESE 2022). For smoothing a Gaussian filter with 12 months long window length was used. The gray area presents the time period covered by the InSAR measurements

geodetic and groundwater level measurements would definitely be a useful tool to study that question in the future.

Another important question for the perspective of city environment and infrastructure is the source (or sources) of such noticeable groundwater level variations with complementing land motion. The annual/interannual fluctuations of groundwater level up to several meters cannot be easily connected with the natural variations, which seems to be about 0.5 m according to the measured water level (Fig. 12). Thus we assumed that some major groundwater pumping event took place in Tallinn in 2016–2017 which was stopped in 2018. According to the observations in well 36 the drop with following recovery of groundwater level occurred earlier (about half a year) than in other wells. Hence, the source of groundwater discharge could be closer to the well 36, and probably eastward of it. However, those assumptions would still need validation, e.g. by applying rigorous hydrogeological modeling complemented with additional hydrological data over the area.

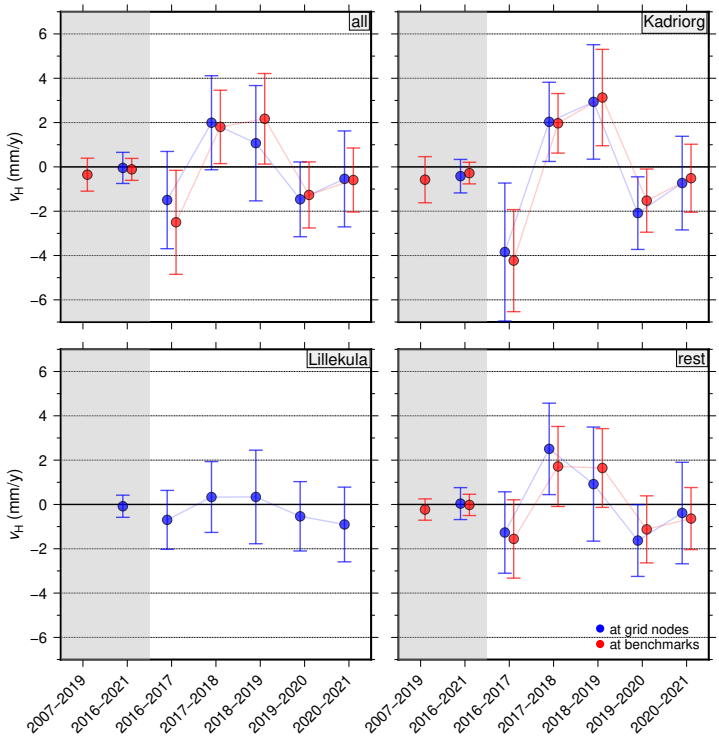

Fig. 12. Mean velocity and the standard deviation of the mean (represented by error bars) was estimated over the nodes of InSAR vertical velocity grids (blue), and the leveled (2007–2019) and InSAR derived velocities at the benchmarks (red). The gray background separates long-term solutions (leveling, InSAR) from yearly solutions (InSAR). The statistics were estimated for all study area (all), Kadriorg and Lilleküla buried valleys, and the rest with valleys excluded, see also Figure 1

For the assessment of spatial correlation between the geological information and the displacements in Tallinn area, the mean and standard deviation of leveled and InSAR velocities at the benchmarks and the grid nodes of velocity models were estimated

(Fig. 12). For that the velocity values were first processed over the full analysis area (includes 116 benchmarks and around 77400 grid nodes), then over the buried valleys of Kadriorg (41 benchmarks, ~ 10400 nodes) and Lilleküla (0 benchmark, ~ 16000 nodes), and finally over the rest of area without buried valleys (75 benchmarks, ~ 50000 nodes).

Firstly, the statistics of the velocity values at the benchmarks and the grid nodes are practically same over different areas. Note that there are no benchmarks over the area of Lilleküla buried valley. Long-term velocities derived from leveling and InSAR analysis are close to zero or show a small negative bias, with higher values in the Kadriorg buried valley. As expected, the mean values of short-term InSAR solutions show subsidence in 2016–2017, the uplift in 2017–2019 and then subsidence again in 2019–2021. The biggest and statistically significant subsidence-uplift pattern was found in Kadriorg. The smallest yearly variations exist in Lilleküla. Accordingly, the largest vertical land movement occurred in the Kadriorg buried valley, but this movement with similar subsidence-uplift pattern extends also to the surrounding areas, even to the Lilleküla buried valley. It is reasonable to think that the source of this movement is linked with the Kadriorg buried valley.

8. Conclusions

The evaluation of millimeter-scale long-term vertical displacements in the Tallinn city center based on repeated leveling in 2007–2019 and InSAR data in 2016–2021 resulted similar subsidence rates. The comparison of long-term vertical velocities at 116 benchmarks of Tallinn height network has shown that the differences between leveled and InSAR results were statistically significant only for the 10% of benchmarks (within 2σ confidence interval). Thus a good agreement between leveled and InSAR derived vertical displacements can be concluded. Furthermore, it illustrates the high efficiency of InSAR measurement technique in monitoring the geodetic infrastructure in urban environment.

InSAR yearly velocity solutions, however, showed 2–3 times higher VLM rates with dominating subsidence in 2016–2017 followed by the uplift in 2018–2019, with relatively stable periods in 2017–2018 and 2019–2021. The historical researches based on repeated leveling have shown that the land subsidence in Tallinn with the largest rates over deep buried valleys was linked with the groundwater level drop due to the excessive water pumping. The significant groundwater level change about −2.5 m in 2016–2017 and 1 m in 2018–2020 observed at three wells in Tallinn seems to support these previous findings. However, the current study presented both the subsidence and uplift of the Tallinn city center, which were found to be temporally coherent with large groundwater level drop followed by some recovery. The statistics of velocity values at the grid nodes of InSAR models and the benchmarks indicated the spatial correlation between the displacements and buried valleys. Accordingly, the current results support the historical findings relied on leveled VLM rates but they also extended the analysis due to the higher spatiotemporal data sampling of InSAR VLM solutions.

Important questions for the future of the city environment and infrastructure of Tallinn are to understand the processes behind the surface deformation, groundwater

level change and their connection with geology. New InSAR analysis complemented with terrestrial geodetic measurements, rigorous hydrogeological modeling and additional geological, hydrological data would be a useful tool to model these processes and further predict the land motion in Tallinn. Further research would also be needed to determine whether the measured displacements were due to the construction activities, some other anthropogenic/natural factor or combination of them.

Author contributions

Conceptualization: T.O. and A.G.; collection and assembly of data: T.O. and A.G.; data analysis and interpretation: T.O.; article writing: T.O.; critical revision and final approval of the article: T.O. and A.G.

Data availability statement

The data that support the findings of this study are available from the corresponding author upon reasonable request.

Acknowledgements

PS-InSAR analysis through SILLE was ordered and financed by Tallinn City. SILLE (www.sille.space) is a satellite-based monitoring and risk measurement service developed and maintained by Datel AS. The authors would like to thank the anonymous reviewers for their constructive comments to improve this article.

References

Crosetto, M., Monserrat, O., Cuevas, M. et al. (2011). Spaceborne differential SAR interferometry: Data analysis tools for deformation measurement. *Remote Sens*., 3, 305–318. DOI: 10.3390/rs3020305.

Estonian Ministry of Environment. (2017). Geodetic system. Legal Acts of Estonia, Decree No. 64. Retrieved May, 2022 from https://www.riigiteataja.ee/akt/128102011003?leiaKehtiv.

Ferretti, A., Prati, C., and Rocca, F. (2001). Permanent scatterers in SAR interferometry. *IEEE Trans. Geosci. Remote Sens.*, 39(1), 8–20. DOI: 10.1109/36.898661.

Fuhrmann, T., and Garthwaite, M.C. (2019). Resolving Three-Dimensional Surface Motion with InSAR: Constraints from Multi-Geometry Data Fusion. *Remote Sens.*, 11, 241. DOI: 10.3390/rs11030241.

GPA (2022). Data retrieved May 11, 2022, from https://gpa.maaamet.ee.

Gruno, A. (2020). *Capabilities of remote sensing on the basis of InSAR data to monitor the Tallinn height network*. Research Report, AS Datel, p. 30.

JCGM (2011). *Evaluation of measurement data. Supplement 2 to the "Guide to the expression of uncertainty in measurement"*. Joint Committee for Guides in Metrology, 102.

Kall, T., and Torim, A. (2003). Vertical movements on the territory of Tallinn. *J. Geodynm.*, 35(4-5), 511–519. DOI: 10.1016/S0264-3707(03)00011-5.

KESE (2022). Data retrieved July, 2022 from https://kese.envir.ee.

Lutsar, R. (1965). *Displacements of the benchmarks of the levelling system network of the city of Tallinn*. Recent Crustal Movements, No. 2, Academy of Sciences of Estonia, Institute of Physics and Astronomy, Tartu. pp. 288–293.

Metricus, O.U. (2019). *Reconstruction of Tallinn height system*. Measurement and adjustment report.

NGL (2021). Data retrieved November, 2021 from http://geodesy.unr.edu/vlm.php.

Perissin, D., Wang, Z., and Wang, T. (2011). Sarproz InSAR tool for urban subsidence/manmade structure stability monitoring in China. In Proceedings of the 34th International Symposium for Remote Sensing of the Environment (ISRSE), Sydney, Australia, 10-15 April 2011.

Smith, W.H.F., and Wessel, P. (1990). Gridding with continuous curvature splines in tension. Geophysics, 55, 293–305. DOI: 10.1190/1.1442837.

Vaher, R., Miidel, A., Raukas, A. and Tavast, E. (2010). Ancient buried valleys in the city of Tallin and adjacent area. *Estonian J. Earth Sci.*, 59(1), 37. DOI: 10.3176/earth.2010.1.03.

Vallner, L., and Lutsar, R. (1966). On the deformations of the earth's surface on the territory of Tallinn. In Proceedings of the Second International Symposium on Recent Crustal Movements. Annales Academiae Scientiarum Fennicae, Series A, III, Geologica-Geographica, 90, Helsinki. pp. 387–394.

Vestøl, O., Ågren J., Steffen, H. et al. (2019). NKG2016LU: A new land uplift model for Fennoscandia and the Baltic region. *J. Geod.*, 93(9), 1759–1779. DOI: 10.1007/s00190-019-01280-8.

Wessel, P., Luis, J.F., Uieda, L. al. (2019). The Generic Mapping Tools version 6. *Geochem. Geophys. Geosystems*, 20, 5556–5564. DOI: 10.1029/2019GC008515.

XGIS (2022). Data retrieved July, 2022 from https://xgis.maaamet.ee/xgis2/page/app/geoloogia50k.

Zhelnin, G. (1958). On the stability of benchmark heights of the levelling system network of the city of Tallinn. *Tartu*, XXXIII (3), 198–218.